Contents lists available at ScienceDirect
Earth and Planetary Science Letters
www.elsevier.com/locate/epsl

Controls on the global distribution of contourite drifts: Insights from an eddy-resolving ocean model

Amanda C. Thran[a,*], Adriana Dutkiewicz[a], Paul Spence[b,c], R. Dietmar Müller[a,d]

[a] EarthByte Group, School of Geosciences, University of Sydney, Sydney NSW 2006, Australia
[b] Climate Change Research Centre, University of New South Wales, Sydney NSW 2052, Australia
[c] ARC Centre of Excellence for Climate System Science, University of New South Wales, Sydney NSW 2052, Australia
[d] Sydney Informatics Hub, University of Sydney, Sydney NSW 2006, Australia

ARTICLE INFO

Article history:
Received 6 December 2017
Received in revised form 25 February 2018
Accepted 27 February 2018
Available online xxxx
Editor: M. Frank

Keywords:
contourite
sediment drift
ocean modelling
meridional overturning circulation
eddy
bottom current

ABSTRACT

Contourite drifts are anomalously high sediment accumulations that form due to reworking by bottom currents. Due to the lack of a comprehensive contourite database, the link between vigorous bottom water activity and drift occurrence has yet to be demonstrated on a global scale. Using an eddy-resolving ocean model and a new georeferenced database of 267 contourites, we show that the global distribution of modern contourite drifts strongly depends on the configuration of the world's most powerful bottom currents. Bathymetric obstacles frequently modify flow direction and intensity, imposing additional finer-scale control on drift occurrence. Mean bottom current speed over contourite-covered areas is only slightly higher (2.2 cm/s) than the rest of the global ocean (1.1 cm/s), falling below proposed thresholds deemed necessary to re-suspend and redistribute sediments (10–15 cm/s). However, currents fluctuate more frequently and intensely over areas with drifts, highlighting the role of intermittent, high-energy bottom current events in sediment erosion, transport, and subsequent drift accumulation. We identify eddies as a major driver of these bottom current fluctuations, and we find that simulated bottom eddy kinetic energy is over three times higher in contourite-covered areas in comparison to the rest of the ocean. Our work supports previous hypotheses which suggest that contourite deposition predominantly occurs due to repeated acute events as opposed to continuous reworking under average-intensity background flow conditions. This suggests that the contourite record should be interpreted in terms of a bottom current's susceptibility to experiencing periodic, high-speed current events. Our results also highlight the potential role of upper ocean dynamics in contourite sedimentation through its direct influence on deep eddy circulation.

1. Introduction

Contourite drifts (or "sediment drifts") are anomalously high accumulations of deep-sea sediment that are largely found around prominent bathymetric obstacles. These features have become frequent ocean drilling targets, as they can preserve high-resolution sedimentological evidence of major paleoceanographic and/or paleoclimatic change (Rebesco et al., 2014). In a series of seminal papers, Heezen et al. (1966) were among the first to propose bottom currents as the main driver for their formation, and the link between contourite drifts and the world's most powerful bottom currents steadily became apparent as more contourite drifts were discovered (Hollister and Heezen, 1972). However, causality between bottom current activity and contourite drift occurrence can be difficult to demonstrate in situ for all cases; these features are often highly inaccessible, and investigators have had to rely on sparse current meter measurements or oceanographic transects to gauge the regional hydrodynamic setting of their survey area (Rebesco et al., 2014). Such methods, though essential for ground-truthing, may not adequately represent the oceanographic processes that lead to drift formation. The use of ocean circulation models can help address these shortcomings, as they simulate these processes on larger scales while abiding by the physical restrictions imposed by fluid dynamics.

In bridging the gap between physical oceanography and the deep-sea sedimentological record, it is becoming more common to present simulation results in tandem with site survey data (e.g., seismic reflection profiling, core analyses, bathymetry data, backscatter intensities, current meter measurements, etc.) as an additional independent line of evidence used to demon-

* Corresponding author.
E-mail address: thran@sydney.edu.au (A.C. Thran).

https://doi.org/10.1016/j.epsl.2018.02.044

strate a given contourite's formation mechanisms (Chen et al., 2016; Hanebuth et al., 2015; Hernández-Molina et al., 2011; Uenzelmann-Neben et al., 2016). Interestingly, numerical simulations have been used to resolve and investigate lesser-known oceanographic processes (e.g., internal waves and dense shelf water cascading) that could be responsible for the formation of many shallow-water, smaller-scale drifts and their associated bedforms (Bonaldo et al., 2016; Droghei et al., 2016; Martorelli et al., 2010; Stow et al., 2009). Nevertheless, a numerical approach to drift occurrence has only been implemented on a regional scale (Bonaldo et al., 2016; Chen et al., 2016; Droghei et al., 2016; Hanebuth et al., 2015; Haupt et al., 1994; Hernández-Molina et al., 2011; Martorelli et al., 2010; Salles et al., 2010), and regional simulations are accompanied by their own set of limitations. Regional computational domains can produce boundary artefacts (Haupt et al., 1994) and generally have trouble realistically representing critical global-scale processes (e.g., Atlantic meridional overturning circulation – AMOC) that are thought to exert first-order control on contourite drift distribution throughout the world's oceans (Rebesco et al., 2014). To date, the absence of a global, cohesive contourite database has prevented the link between large-scale ocean circulation patterns and contourite drift occurrence to be demonstrated. In this paper, we present a census of the world's known contourite features and use the database to assess the relationship between simulated bottom current activity and contourite distribution throughout the ocean. This work represents one part of a growing effort to unite numerical methods with observations from the geological record.

2. Methods

2.1. Distribution of modern contourites

An exhaustive review of the literature was conducted to assess and refine the known coverage of modern sediment drifts. Two major existing databases were used as a basis for compiling the distribution of contourites used in this study. The first database was presented by Rebesco et al. (2014) in their recent review of contourites, and this was merged with a second online database curated by the Flanders Marine Institute (Claus et al., 2017). Additionally, more recently reported features were added to these merged databases (see Supplementary Table S1). The spatial extent of each feature was carefully re-assessed and modified by georeferencing maps provided in the original sources, as a particularly high level of granularity was required for the application of a high resolution, eddy-resolving ocean circulation model. We relied heavily upon the interpretations of the original authors, where distinct contourite geometries and morphologies (e.g., asymmetrical mounds, moats, sediment waves, erosional bedforms) were interpreted from sub-bottom profiles, multibeam and side-scan sonar data, backscatter data, and seafloor photographs. Features were omitted if they were identified solely based on core descriptions or if they are presently buried beneath turbidites or uniform hemipelagic drapes. Although aimed to be exhaustive, this compilation of known sediment drifts is a work in progress as we anticipate that many more features will be reported in the future.

2.2. Global ocean sea-ice model

To simulate present-day bottom current activity, we use a global ocean–sea ice model (MOM01) that is based on the Geophysical Fluid Dynamics Laboratory (GFDL) CM2.6 coupled climate model (Griffies et al., 2015). The model has a mesoscale eddy resolving 0.1° Mercator horizontal resolution with 75 vertical levels, where the vertical grid was engineered to resolve deep ocean eddies (Stewart et al., 2017). The model was equilibrated for 70 years to reach a dynamically steady state. The atmospheric forcing is prescribed from version 2 of the Coordinated Ocean–ice Reference Experiments (CORE) data (Griffies et al., 2009). The model accurately represents global bathymetric features and realistically simulates the critical drivers of bottom flows (e.g., global meridional overturning circulation – MOC, wind-driven shallow-water circulation, eddy transport, etc.) associated with sediment drift formation (Rebesco et al., 2014).

Simulated bottom current metrics (e.g., time-mean and maximum current speeds, and speed standard deviation) were then examined in relation to the distribution of contourite drifts. Simulated eddy kinetic energy in the model's bottom layer was also considered, where eddy kinetic energy was computed by decomposing daily velocity field outputs into their mean and eddy components, following the methods of Stewart et al. (2017). For each metric, values were extracted from all contourite-covered areas (i.e., points that lie within the bounds of the contourite polygons) using a Hierarchical Equal Area isoLatitude Pixelization (HEALPix) mesh of similar resolution to the computational domain at the equator (Gorski et al., 2005). Extraction of these bottom current metrics was repeated for all points that comprise the global ocean.

When discussing modelled bottom currents, where possible we provide the current name or alternatively specify the large-scale water mass classification on the basis of previous work. Identifying regional-scale intermediate and deep-water masses requires a rigorous examination of the computed vertical stratification of the water column, and thus lies beyond the scope of the study.

3. Results

3.1. Bottom current activity and global contourite distribution

The most energetic bottom currents are simulated along the western boundaries of ocean basins, near deep water creation sites, and in areas that are tightly constricted by topography. Such regions are associated with higher computed bottom current metrics (i.e., mean and maximum annual bottom current speed and bottom current speed standard deviation). There is substantial overlap between these metrics; generally, areas of the ocean with the highest mean annual bottom current speeds (U_{mean}; Fig. 1A) also exhibit the highest maximum simulated speeds (U_{max}; Fig. 1B) and standard deviation values (U_{std}; Fig. 1C).

Areas with stronger simulated bottom current activity closely correspond to the global distribution of 267 contourite features compiled from published literature (Fig. 1, see Supplementary Table S1). The average mean annual bottom current speed computed for all contourites (130,685 total computed points, ~6.3 km resolution) is 2.2 cm/s. This double that of the total global ocean, where mean annual bottom current speeds are 1.1 cm/s on average (based on 8,789,594 total computed points). Violin plots show similar kernel density distributions for computed mean annual speeds in both contourite-covered areas and the total global ocean (Fig. 2A). There is variation between the kernel density distributions when contourite coverage is grouped by region. Naturally, regions with particularly intense bottom currents exhibit a wider range of mean annual current speeds. Southwest Pacific contourites experience the highest speeds on average ($U_{mean} = 2.7$ cm/s) while contourites in the eastern North Atlantic (i.e., the Iberian Peninsula) experience the lowest ($U_{mean} = 0.7$ cm/s). Overall, contourites are found in areas of the seafloor where simulated mean annual bottom currents speeds are less than 10 cm/s.

In contrast to the mean annual bottom current speed, simulated maximum annual bottom current speeds achieve higher values in contourite-covered areas as compared to the global ocean (Fig. 2B). On average, maximum speeds in contourite-covered areas reach 15 cm/s, whereas the global ocean experiences maximum

Please cite this article in press as: Thran, A.C., et al. Controls on the global distribution of contourite drifts: Insights from an eddy-resolving ocean model. Earth Planet. Sci. Lett. (2018), https://doi.org/10.1016/j.epsl.2018.02.044

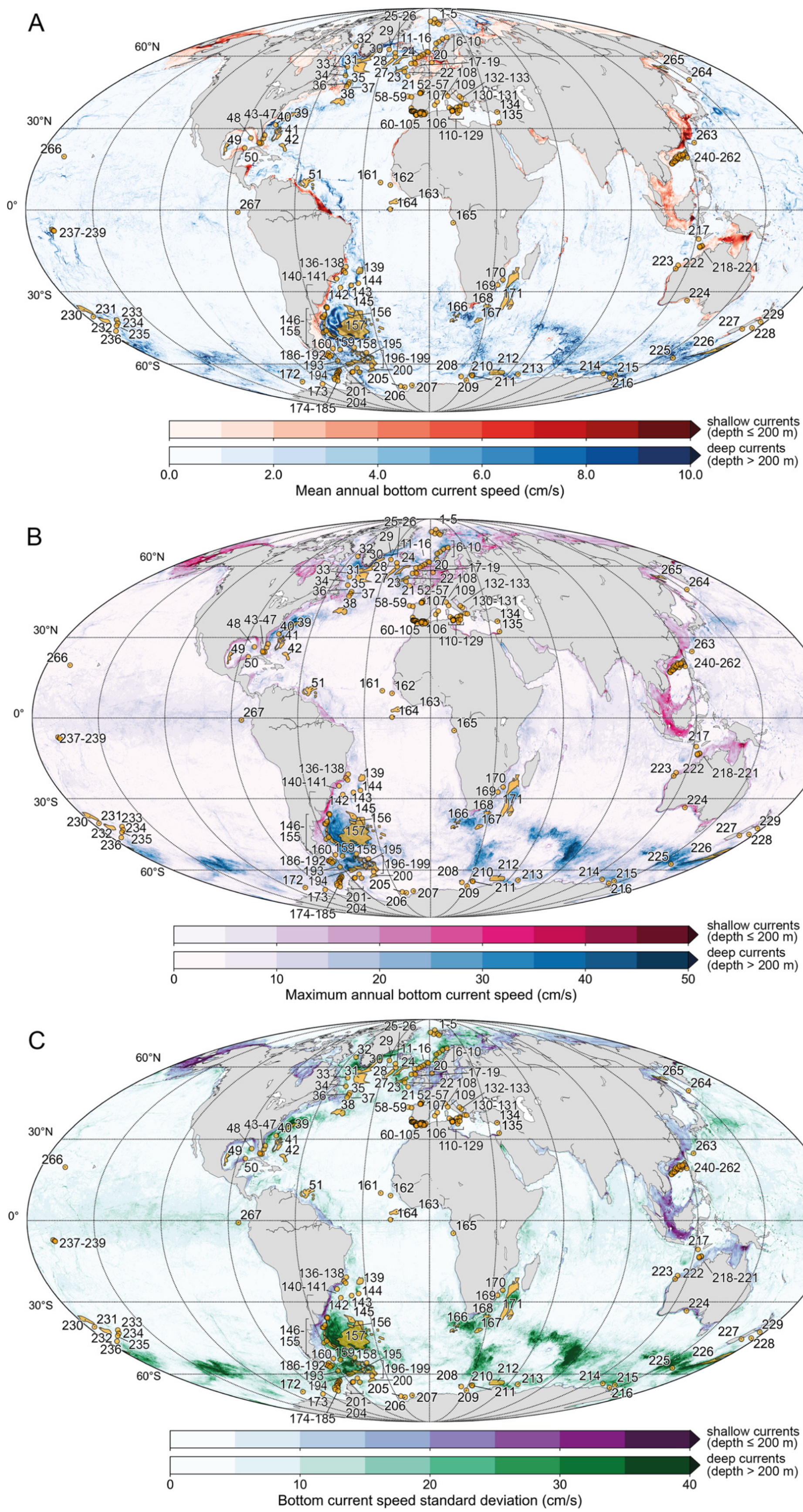

Fig. 1. Global distribution of modern contourite drifts overlying simulated mean annual (A), maximum annual (B), and annual standard deviation (C) for bottom current speeds. Smaller contourites are represented as points. Warmer colours are indicative of shallow (typically shelf-confined) bottom currents (depth ≤200 m) whereas cooler colours indicate deeper bottom currents (depth >200 m). Number labels correspond to the index given in Table S1 of contourite attributes (Tab. S1). Molleweide projection. Q3 (For interpretation of the colours in the figure(s), the reader is referred to the web version of this article.)

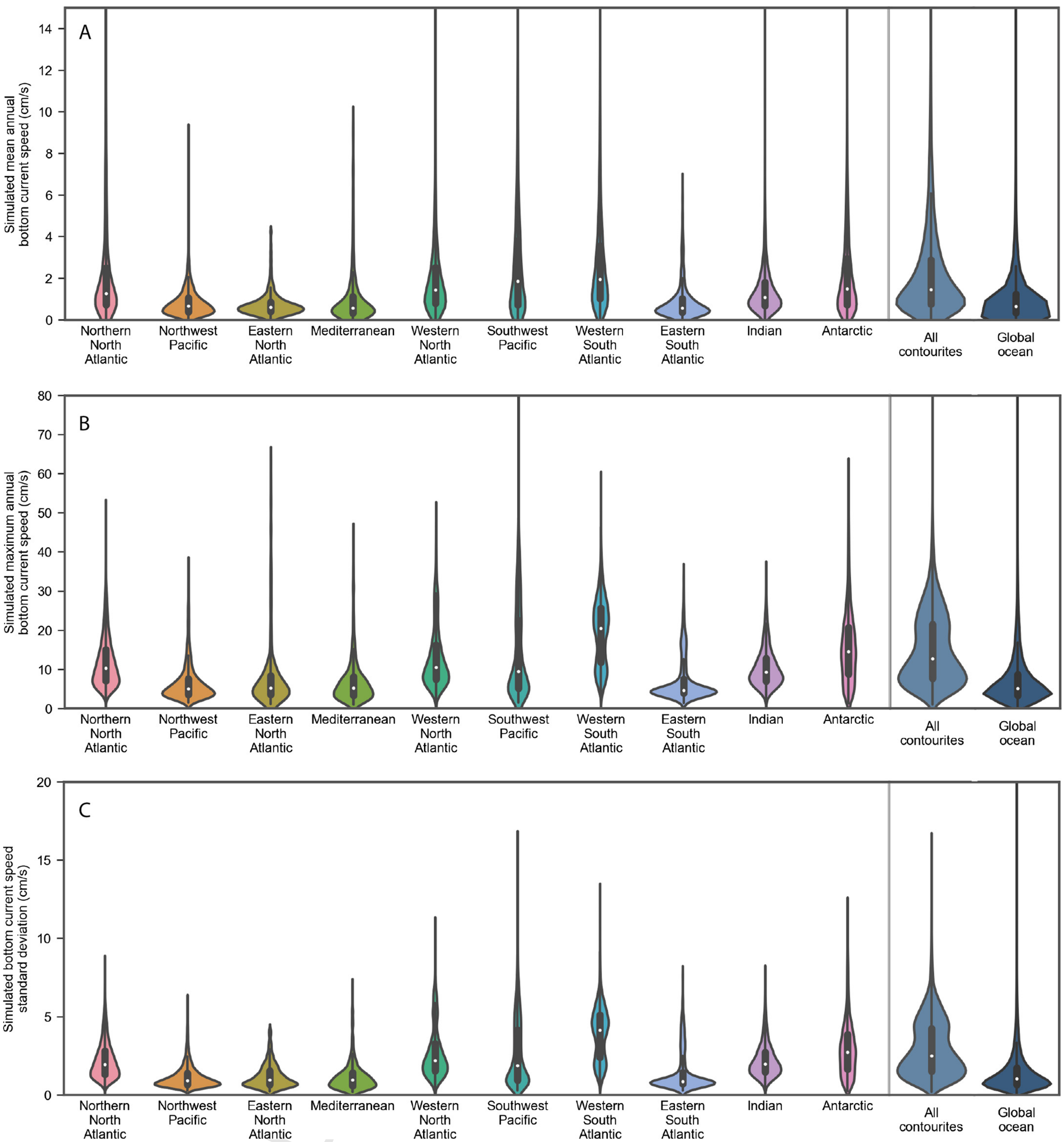

Fig. 2. Violin plots showing kernel density distributions of computed average annual bottom current speed (A), maximum annual speed (B), the standard deviation (C) for contourite coverage in their respective regions, total contourite coverage, and the global ocean. Note the markedly different distributions between contourite-covered areas and the global ocean for the maximum speed and standard deviation metrics 2B and C). Contourites in the eastern Pacific were excluded from this plot due to scarce coverage. Plots were truncated where outliers comprised less than 0.01% of all computed points.

speeds of 7.3 cm/s on average. Violin plots of the frequency distribution of computed maxima show markedly different distributions for contourite-covered areas, where the range of maximum speeds found over contourites is larger than that of the global ocean. Simulated maximum bottom current speeds typically do not exceed 50 cm/s in areas with contourites. On average by region, the western South Atlantic exhibits the highest computed currents speeds whereas the Northwest Pacific has the lowest. Bottom current speed standard deviations follow a similar trend (Fig. 2C), where the contourite average is 2.9 cm/s, double the global average of 1.4 cm/s, and the kernel density distribution covers a wider range of standard deviations for contourite-covered areas.

When grouped on an individual feature basis, a wider range of mean annual computed bottom current speeds are computed for

Please cite this article in press as: Thran, A.C., et al. Controls on the global distribution of contourite drifts: Insights from an eddy-resolving ocean model. Earth Planet. Sci. Lett. (2018), https://doi.org/10.1016/j.epsl.2018.02.044

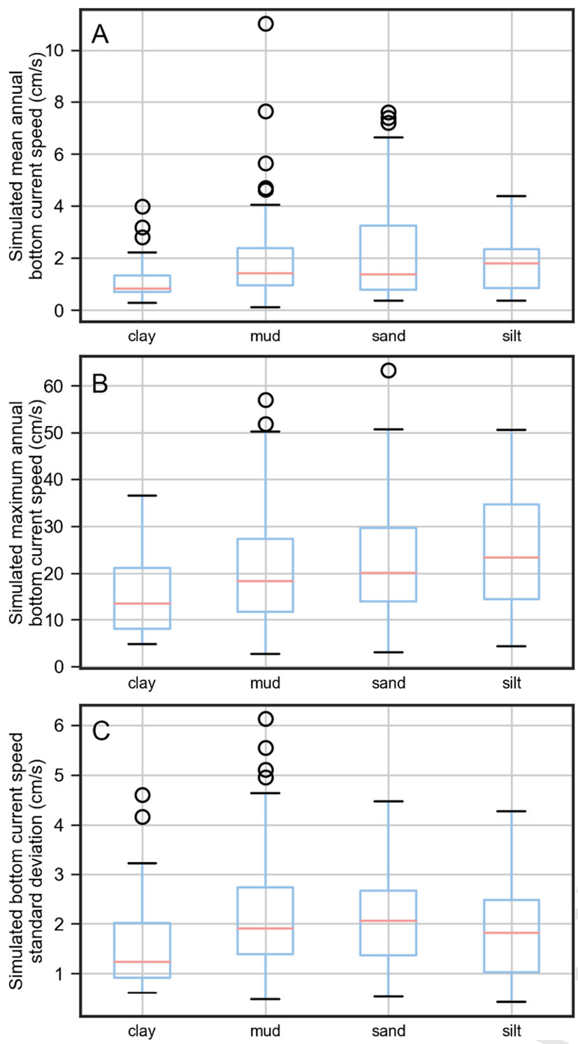

Fig. 3. Boxplots depicting computed mean annual bottom current speeds (A), maximum annual bottom current speeds (B), and bottom current speed standard deviation (C) for individual contourite features, grouped by principle grain size classification (see Supplementary Table S1). Circles indicate features that are outliers.

contourites that are principally composed of sand (Fig. 3A), where ranges narrow as grain size decreases. Notably, clayey contourites occupy a tight range of bottom current speeds and are absent from areas that experience mean annual values >4 cm/s. Similar trends are obtained for computed maximum speeds (Fig. 3B), although silty contourites exhibit a slightly higher computed median and a wider range than the other principle grain-size categories. Finally, the range of standard deviation values (Fig. 3C) computed for predominantly sandy and muddy contourites are widest with the highest medians. Silty contourites have a similar size range and a slightly lower median, and clayey contourites have the lowest median and range.

Global contourite coverage appears to correspond to high simulated mean bottom eddy kinetic energy ($\overline{EKE}$; Fig. 4A). On average, eddy kinetic energy is 17.5 $cm^2\,s^{-2}$ for contourite-covered areas and 5.3 $cm^2\,s^{-2}$ for the global ocean. Additionally, violin plots indicate a wider range of eddy kinetic energy values extracted from contourite-covered areas compared to the global ocean (Fig. 4B). Eddy kinetic energy for contourite-covered areas varies depending on region, with western South Atlantic contourites exhibiting the highest computed eddy kinetic energies ($\overline{EKE} = 29.2$ $cm^2\,s^{-2}$) and the eastern North Atlantic experiencing the lowest eddy kinetic energies on average ($\overline{EKE} = 2.3$ $cm^2\,s^{-2}$).

To summarize a few main findings from the database, computed drift areas range from 1 to > 1 × 10^6 km^2 and exhibit a diverse range of morphologies (see Table S1). Of all the contourites with valid maximum age estimates (218 features), one is Palaeocene (<1%), six are Eocene (∼2.8%), 10 formed at the Eocene-Oligocene transition (∼4.6%), 21 are Oligocene (∼9.8%), 80 are Miocene (∼37%), 30 are Pliocene (∼14%), four formed at the Plio-Pleistocene transition (∼1.8%), and 64 are Quaternary (∼29%).

3.2. Regions of interest

A regional plot of the bottom layer's velocity field and standard deviation in the northern North Atlantic (Fig. 5A) reveals the meandering, topographically-regulated trajectory of the AMOC, where the Iceland–Scotland Overflow Water (ISOW) and the Deep Western Boundary Current (DWBC) transport recently formed North Atlantic Deep Water (NADW) southward (Hunter et al., 2007). The simulated currents with the higher standard deviation values coincide with a series of well-known, prominent North Atlantic drifts, many of which have long been associated with AMOC transport (Heezen et al., 1966; McCave and Tucholke, 1986; Rebesco et al., 2014; Wold, 1994). The shallow Norwegian Current, which travels northward and branches into the West Spitsbergen Current, flows over young, smaller, slope-confined and infill drifts along the Norwegian continental slope and the larger Spitsbergen drift complex (Rebesco et al., 2013). The area covered by the Gloria Drift (Fig. 5A – #31; Egloff and Johnson, 1975) yields notably slow computed bottom current speeds ($U_{std} = 1.3$ cm/s).

Further southwest in the Western North Atlantic (Fig. 5B), the simulated DWBC continues its path along the Canadian continental margin and flows over the smaller drifts that rim the Flemish Cap. The DWBC (or more commonly in this region, the Western Boundary Undercurrent), which entrains NADW, then travels southwest along the Canadian and eastern United States continental margin, where it is overlaid by the intense poleward flowing Gulf Stream. In this region (Fig. 4B – #38–40), Gulf Stream meanders spawn cyclonic and anticyclonic eddies that affect both the NADW and the Antarctic Bottom Water (AABW) that lies directly beneath it (Gardner et al., 2017), inciting highly variable bottom currents over the Hatteras wave field (Fig. 5B – #39) and other expansive bottom-reworked sediments that reside on the abyssal plain (McCave and Tucholke, 1986). A northwest-flowing intrusion of Antarctic Bottom Water (AABW) is thought to interact with NADW along the northeast South American continental margin (Mauritzen et al., 2002), where there are drift complexes on the Demerara Rise (Fig. 5B – #51) and the Greater Antilles Outer Ridge (Fig. 5B – #42). Further west towards the continents, the Loop Current, along with its associated rings, produces vigorous bottom current activity in the Gulf of Mexico and funnels surface waters through the Straits of Florida (propelling the Antilles Current and Florida Current) past a cluster of carbonate drifts ($U_{max} \approx 40$ cm/s).

In the Mediterranean region (Fig. 5C), contourite deposition is well-documented and often predominantly tied to the production and subsequent departure of the intermediate Mediterranean Outflow Water (MOW) through the narrow Strait of Gibraltar and into the Gulf of Cádiz, where they extensively line the Iberian Peninsula's continental slope (Hernández-Molina et al., 2011). In and around the Strait of Gibraltar, currents deviate considerably from the mean and coincide with contourite coverage ($U_{max} \approx 65$ cm/s). Drifts are found in the Adriatic Sea and the Gulf of Lion, where various dense water masses (e.g., North Adriatic Dense Water – NAdDW) are created and influence the bottom current regime (Millot, 1999). The Strait of Sicily accentuates the flow of dense water masses created towards the east in the Levantine Sea and is inhabited by many contourites (e.g., Fig. 5C – #111). Simulated surface currents (e.g., Levant Jet) similarly coincide with shallow

Please cite this article in press as: Thran, A.C., et al. Controls on the global distribution of contourite drifts: Insights from an eddy-resolving ocean model. Earth Planet. Sci. Lett. (2018), https://doi.org/10.1016/j.epsl.2018.02.044

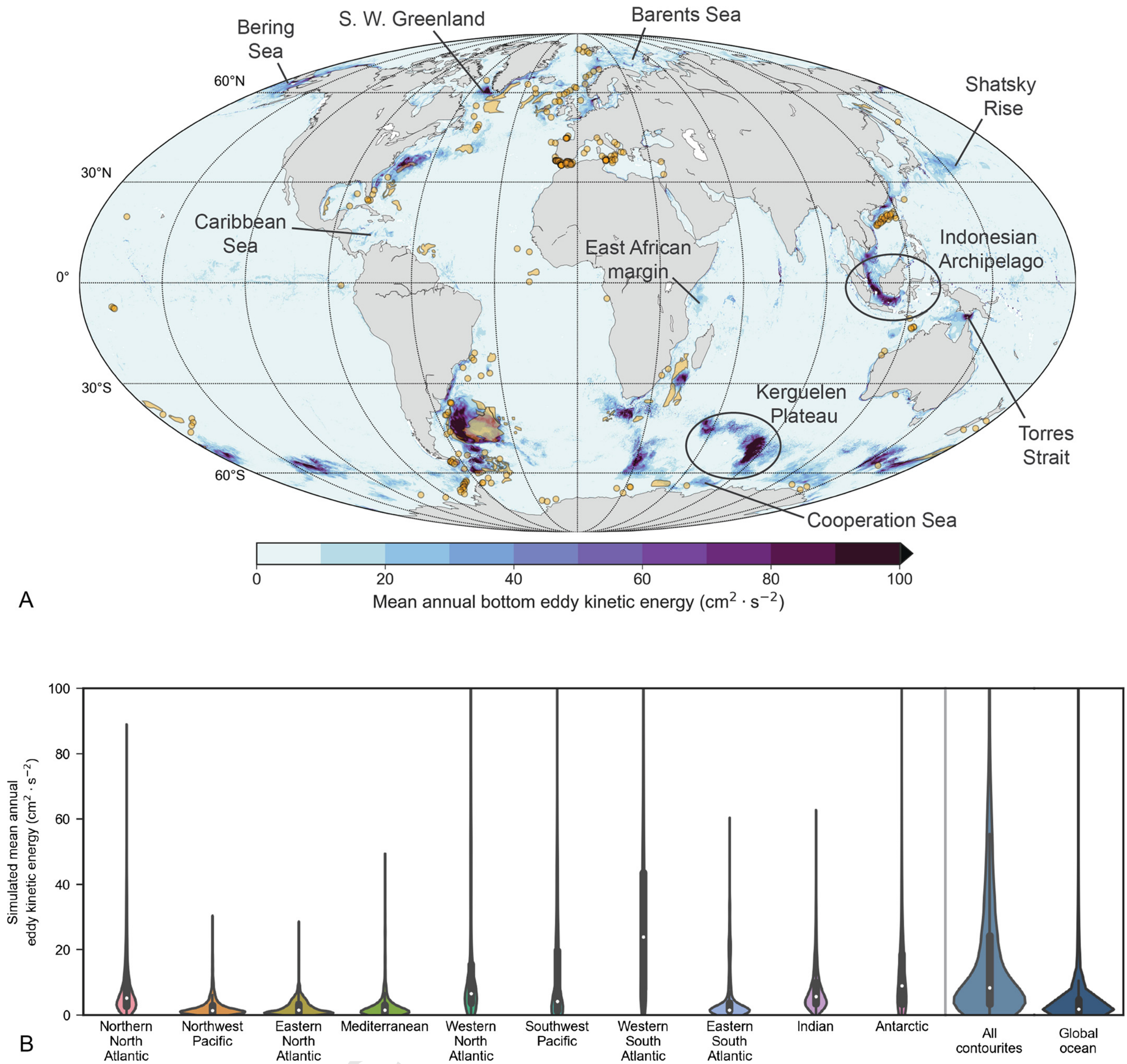

Fig. 4. (A) Simulated mean annual eddy kinetic energy distribution in the bottom layer of the model. Also annotated are regions that potentially contain presently-undiscovered modern drift coverage (see Section 4.5). (B) Violin plots showing kernel density distributions of eddy kinetic energy values extracted from respective contourite regions, all contourite-covered areas, and the global ocean. Plots were truncated where outliers comprised less than 0.01% of all computed points.

contourite formation throughout the Mediterranean (Schattner et al., 2015).

Vigorous bottom currents are simulated in the Western South Atlantic (Fig. 6A), which hosts a series of well-studied contourite depositional systems. Along the South American continental margin, the simulated shallow Brazil Current and the Falkland Current flow over a series of drifts on the continental slope and rise (Hernández-Molina et al., 2009). Highly energetic bottom currents are simulated at the Brazil–Malvinas Confluence and into the deep Argentine Basin, which houses the Zapiola sediment wave field (Fig. 6A – #157, Flood and Shor, 1988). Broadly speaking, high simulated current speeds in the deeper parts of this region likely reflect the local intensification of a handful of intermediate and deep-water masses originating from Antarctica (principally, AABW), along with a southward-flowing branch of the NADW (Flood and Shor, 1988; Hernández-Molina et al., 2009). Additionally, a strand of AABW (also seen in the western North Atlantic – Fig. 5B) flows northeast over a series of drifts that lie further from the margin (Faugères et al., 2002).

Simulated current speeds in the eastern South Atlantic (Fig. 6B) are generally low and contourite drift occurrence is almost exclusively confined to southern Africa, where the Agulhas Current and its associated rings are simulated. Flow is slightly constricted through the Mozambique Channel and leads to relatively high speeds, where various sediment wave fields and erosional bedforms have been mapped in this area (Breitzke et al., 2017).

Circulation in the Southern Ocean (Fig. 6C) is highly complex and involves various water masses. Generally speaking, energetic bottom currents simulated throughout the Southern Ocean demonstrate the activity of the ACC, which is largely steered by

Please cite this article in press as: Thran, A.C., et al. Controls on the global distribution of contourite drifts: Insights from an eddy-resolving ocean model. Earth Planet. Sci. Lett. (2018), https://doi.org/10.1016/j.epsl.2018.02.044

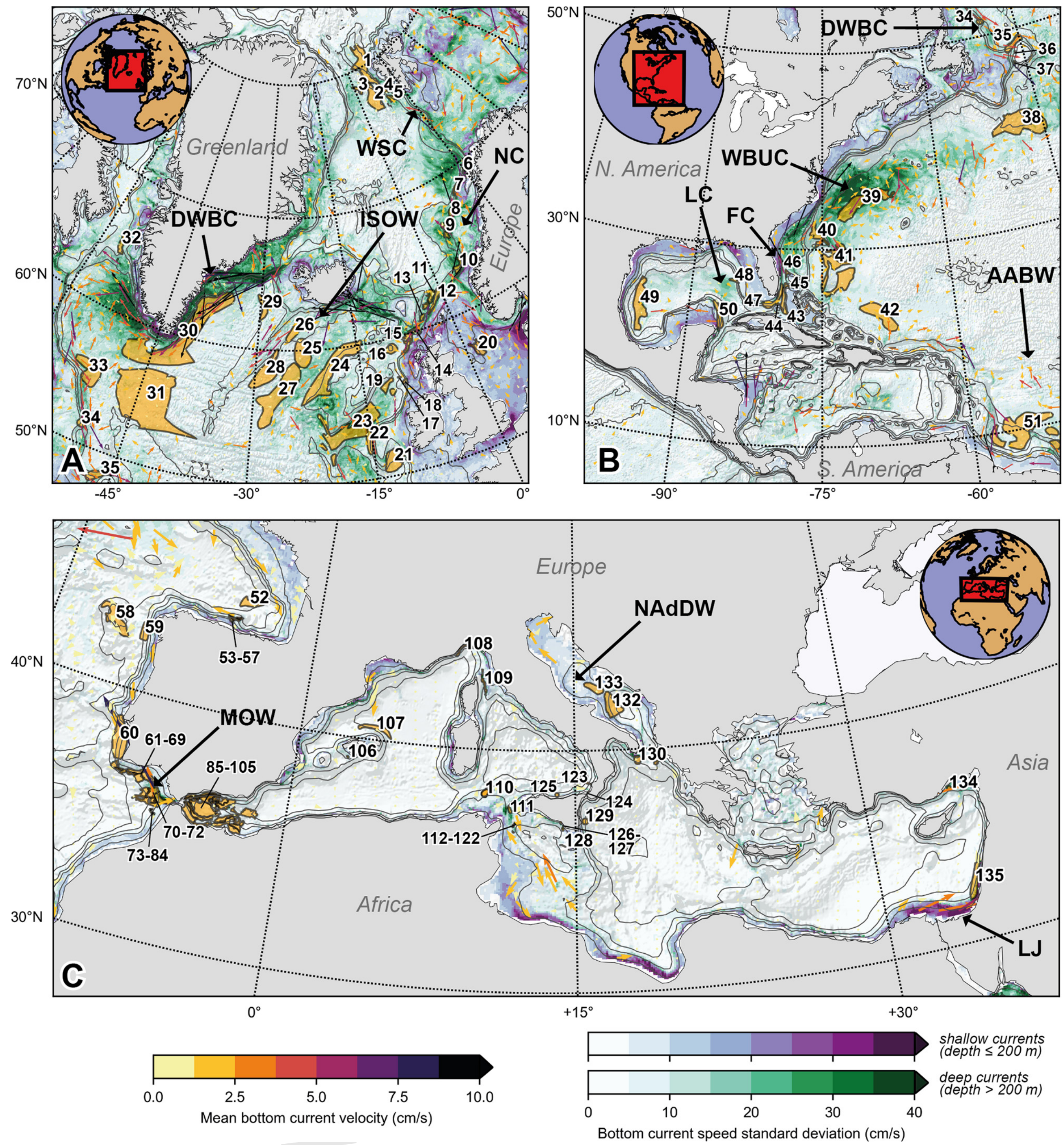

Fig. 5. Regional-scale distribution of contourite drifts for the northern North Atlantic (A), western North Atlantic (B), Mediterranean (C). Contourites are overlying standard deviation of annual computed bottom current speeds (U_{std}), with quivers indicating the computed mean annual velocity field. Number labels correspond to the index given in Supplementary Table S1. Principle currents and/or water masses include: DWBC = Deep Western Boundary Current, WSC = West Spitsbergen Current, NC = Norwegian Current, ISOW = Iceland-Scotland Overflow Water, WBUC = Western Boundary Undercurrent, LC = Loop Current, FC = Florida Current, AABW = Antarctic Bottom Water, MOW = Mediterranean Outflow Water, NAdDW = Northern Adriatic Dense Water, LJ = Levant Jet. All plots presented using a Lambert Conformal Conic projection.

bathymetry (Orsi et al., 1995). AABW, which originates along the Wilkes Land Margin, in the Ross Sea, and in the Weddell Sea (where it is referred to as Weddell Sea Deep Water), flows equatorward via a series of deep boundary currents. Several drifts rim the Antarctic margin, with a large concentration of features in and around the Drake Passage (Pérez et al., 2015). The Drake Passage is one of the world's most important ocean gateways and accentuates the flow of the ACC ($U_{\max} \approx 90$ cm/s), leading to locally high and variable bottom current speeds (Orsi et al., 1995). West of the Antarctic Peninsula, a SW-flowing countercurrent is reproduced over a series of well-known drifts (#174–#185; Hillenbrand et al., 2008).

The majority of large, deep sediment drifts in the Oceania region (Fig. 7A) are concentrated to the east of New Zealand in the Southwest Pacific gateway (Carter et al., 2004), where the Pacific DWBC is simulated. Other shallow-water drifts are found rimming the NW Australian continental margin beneath simulated shelf currents and in the Sumba Basin (#217, Fig. 7A). In the Northwest Pacific (Fig. 7B), relatively mild bottom currents are simulated over a large cluster of small contourite drifts in the South China Sea

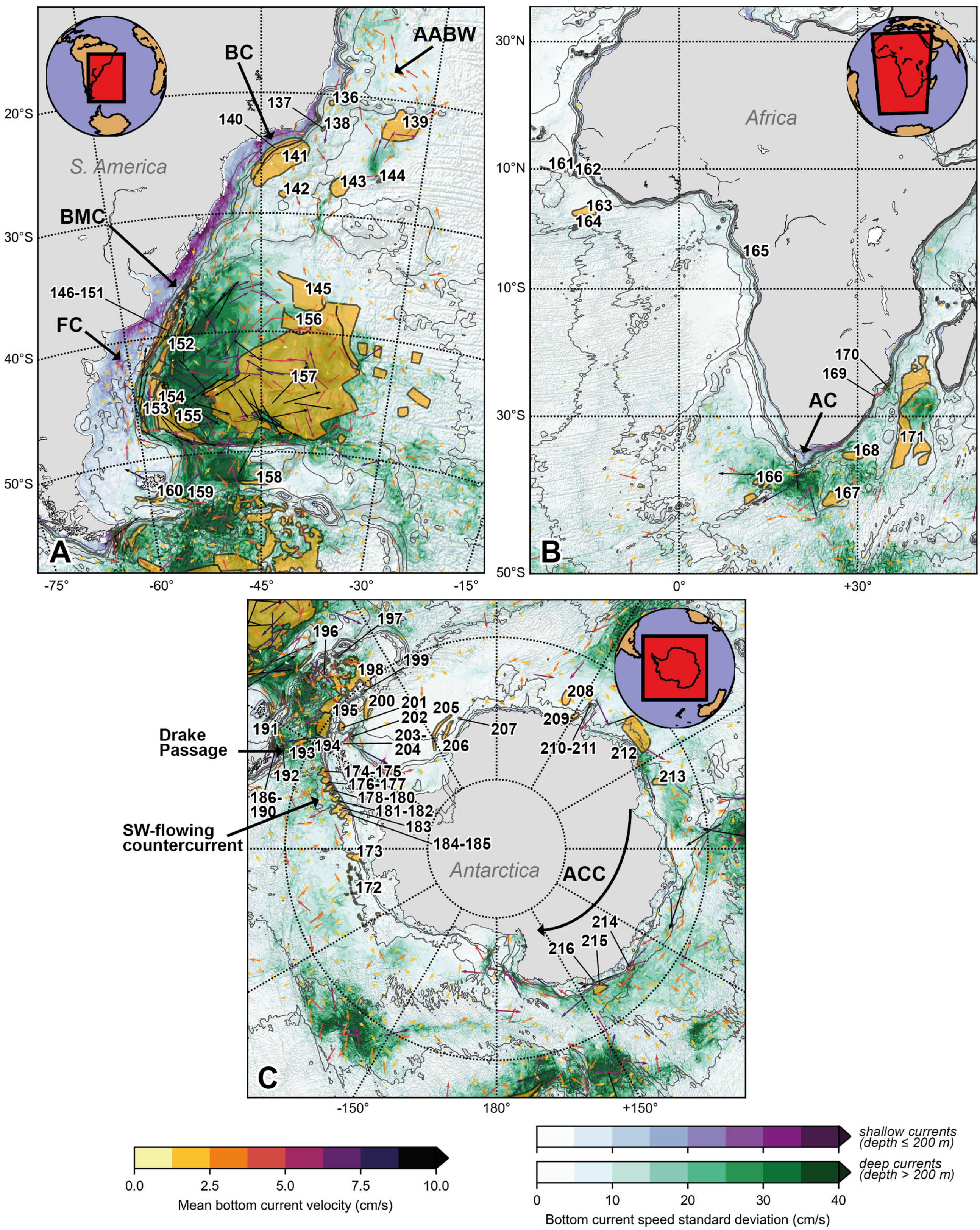

Fig. 6. Regional-scale distribution of contourite drifts for western South Atlantic (A), eastern South Atlantic (B), Southern Ocean (C). Contourites are overlying standard deviation of annual computed bottom current speeds (U_{std}), with quivers indicating the computed mean annual velocity field. Number labels correspond to the index given in Supplementary Table S1. Plots presented using Lambert Conformal Conic (A), Mercator (B), and Polar Stereographic (C) projections. Principle currents and/or water masses include: AABW = Antarctic Bottom Water; BC = Brazil Current, BMC = Brazil-Malvinas Confluence, FC = Falkland Current, AC = Agulhas Current, ACC = Antarctic Circumpolar Current.

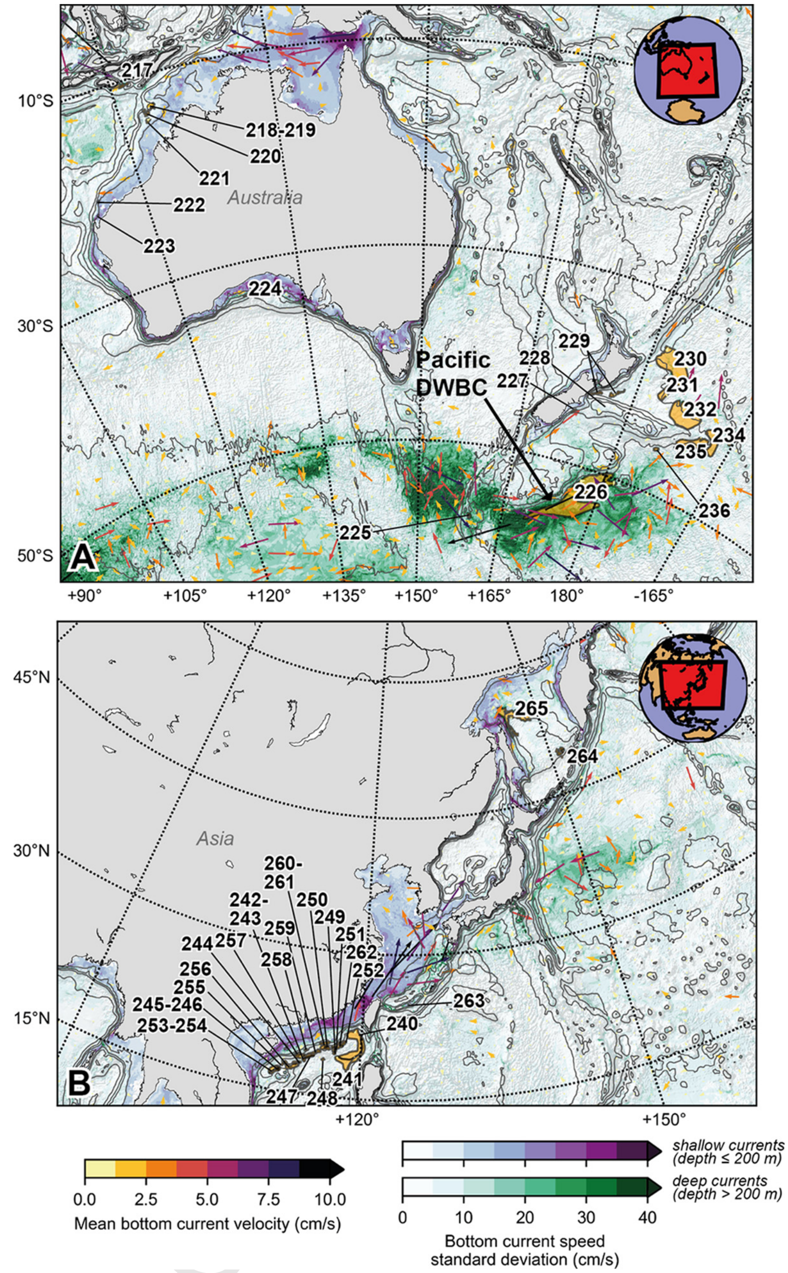

Fig. 7. Regional-scale distribution of contourite drifts for Oceania (A), and the Northwest Pacific (B). Contourites are overlying standard deviation of annual computed bottom current speeds (U_{std}), with quivers indicating the computed mean annual velocity field. Number labels correspond to the index given in Supplementary Table S1. Both plots presented using a Lambert Conformal Conic projection. Principle water mass includes: DWBC = Deep Western Boundary Current.

(Li et al., 2013), though strong surface currents are simulated on the shelf. Standard deviations are high over a large drift in the Sea of Okhotsk (#265, Fig. 7B), which is thought to be a site of Sea of Okhotsk Intermediate Water formation (Wong et al., 2003).

4. Discussion

4.1. Global outlook

The close overlap between global modern contourite distribution and vigorous simulated bottom current activity (Fig. 1) reaffirms the widely-held view that the global MOC exerts a first-order control on contourite distribution (Rebesco et al., 2014). Contourites are disproportionately common on the western sides of ocean basins, which is consistent with the modern configuration of the most vigorous currents. Western intensification of wind-driven currents encourages higher speeds in shallow areas, whereas the Coriolis effect deflects water masses against the topographic boundaries imposed by the continents in deep areas, resulting in intense western boundary undercurrents (McCave and Tucholke, 1986). Bathymetric obstacles (e.g., seamounts, channels, ridges) locally redirect and accentuate flow, resulting in smaller-scale drift features. While topography strongly regulates the occurrence and configuration of powerful bottom currents (and, by extension, contourites), our simulations demonstrate that vigorous bottom current activity can occur in areas that are relatively unconstrained by obstacles (e.g., the Argentine Basin), where these areas often coincide with major sediment wave fields (e.g., the Zapiola and Hatteras wave fields). We note that while sediment wave fields are not contourites in the strictest sense (Rebesco et al., 2014), sediment waves nonetheless fall under the continuum of surficial "bottom-reworked bedforms" that are often recognized

Please cite this article in press as: Thran, A.C., et al. Controls on the global distribution of contourite drifts: Insights from an eddy-resolving ocean model. Earth Planet. Sci. Lett. (2018), https://doi.org/10.1016/j.epsl.2018.02.044

in studies of drift formation and occurrence (Rebesco et al., 2014; Stow et al., 2009), and thus have been included in the present assessment. We also note that contourite coverage suggests a strong sampling bias in the Atlantic and Mediterranean in comparison to other areas with considerably high bottom current activity and fewer reported features.

Regional velocity fields reveal that average mean flow rarely manifests as extensive, continuous, unidirectional stream with the exception of a few notable cases (e.g. the DWBC; Fig. 5). In most scenarios, flow is frequently interrupted and reoriented. While partially due to bathymetric obstacles, this also reflects the meandering behaviour of currents and the interaction of transient eddies (Fukamachi et al., 2010; Spence et al., 2012).

4.2. The potential role of eddies in contourite sedimentation

Our results suggest that temporally-persistent ambient current flow may not be the most important driver of contourite formation. Mean annual bottom current speeds, which better represent predominant background flow, are marginally higher for contourite-covered areas (2.2 cm/s) in comparison to the global ocean (1.1 cm/s; Fig. 2A). Numerically simulated mean values from this model, though slightly lower, echo mean current speed measurements for the DWBU at subtropical latitudes (e.g. Bower and Hunt, 2000), where contourites are known to form. Both simulated and measured mean values fall below proposed velocity thresholds required for reworking silt-sized grains (i.e., ∼10–15 cm/s; McCave and Hall, 2006), suggesting that contourite formation should not occur under such conditions. This echoes the findings of Gardner et al. (2017), who propose that mean flows in the DWBC are rarely sufficiently high to entrain sediment and cause the generation of dense nepheloid layers observed in this area.

On the other hand, contourite covered areas begin to differentiate from the global ocean when the maxima and standard deviations for computed bottom current speeds are considered (Fig. 2B and 2C). On average, the maximum speeds over contourites surpass proposed thresholds necessary for sediment remobilisation (15 cm/s) and are much higher than for the rest of the seafloor (7.3 cm/s). Additionally, violin plots indicate that bottom current speeds in contourite-covered areas fluctuate significantly more than those in the global ocean (Fig. 2C). These metrics better reflect the occurrence of transient, more extreme fluctuations in bottom current intensity, which are thought to play a critical role in creating dense nepheloid layers that resuspend sediments (i.e., benthic storms; Gardner et al., 2017; Hollister and McCave, 1984). Our findings support previous hypotheses which propose that contourite formation occurs predominantly due to acute, high-energy bursts of bottom water activity followed by subsequent deposition under relatively low ambient flow conditions (Bonaldo et al., 2016; Breitzke et al., 2017; Hanebuth et al., 2015; Hollister and McCave, 1984).

The high-resolution ocean-sea ice model used in this study was engineered so that both the vertical and horizontal grids fully resolve the first order baroclinic mode in the deep ocean. In particular, this ensured that the vertical grid is capable of resolving mesoscale increases in eddy kinetic energy throughout the water column (up to 200% increase on and surrounding the Antarctic continental shelf and slopes; Stewart et al., 2017). Consequently, eddy-driven horizontal flows in the bottom layer are better captured in the model, owing to the large fluctuations in bottom current velocities. Field measurements beneath the Gulf Stream have confirmed the vertical coherence of such flows to the base of the abyssal plain (depth >5000 m), which surpasses the maximum depth range for the DWBC (Andres et al., 2016). Globally, high eddy kinetic energy in the bottom layer appears to closely correspond to contourite coverage (Fig. 4A), wherein values are three times larger on average ($\overline{EKE} = 17.5\ \text{cm}^2\,\text{s}^{-2}$) in comparison to the rest of the ocean ($\overline{EKE} = 5.3\ \text{cm}^2\,\text{s}^{-2}$). We therefore identify high eddy kinetic energy as a potential control on the global distribution of contourites. Previous regional studies that utilize both wave tanks, current measurements, and eddy-resolving numerical models have also identified meso-scale or sub-meso-scale eddies as a major cause of intermittent high near-bed current speeds, and thus, sediment erosion and subsequent re-deposition in the form of contourite drifts and other bedforms (Gardner et al., 2017; Hanebuth et al., 2015; Martorelli et al., 2010; Stow et al., 2002; Zhang et al., 2016). The role of eddies was also strongly advocated by Gardner et al. (2017) in their study of benthic storms.

4.3. Implications for interpreting the deep sea sedimentological record

The results from our study carry implications for how bottom current intensity should be interpreted from contourites. Firstly, field data indicate that benthic storms occur frequently (∼10 times per year) and operate on short temporal scales, with the period of significant re-suspension lasting several days to weeks (Gardner et al., 2017; Gross and Williams, 1991). Such evidence suggests that the majority of deep-sea sediment reworking throughout the year occurs during relatively short-lived events. The highest sedimentation rates for Quaternary-age contourite drifts are in the order of >100 cm/kyr (e.g., the Nyk Drift; Laberg et al., 2001). Therefore, the ability of the sedimentological record to resolve individual events, especially given the deleterious effect of bioturbation on laminated beds (Rebesco et al., 2014), remains an open question. However, this work demonstrates that large-scale ocean currents have a greater propensity for more variable fluctuations in current speed (and higher bottom eddy kinetic energy) in comparison to the global ocean (Fig. 1). Therefore, it is reasonable to surmise that shifts in general bottom current intensity occur over geological timescales, and that such shifts can still be gleaned from geological record through traditional techniques such as seismic imaging and sediment core analysis. Nevertheless, it may be more precise (and perhaps overly-precise) to conclude that a given current system has undergone a shift in susceptibility to acute, high-speed current events. In other words, a drift is a sedimentological manifestation of repeated instances where critical speed thresholds have been surpassed and sediment has been consequently redeposited.

Secondly, a number of contourite-covered areas are associated with the eddy rich western boundary currents (i.e the Gulf Stream, the Agulhas Current, the Brazil–Malvinas Confluence over the Argentine Basin), and the ACC (Fig. 4) that all have vigorous bottom current fluctuations. A link between these intense surface currents, deep reaching eddy activity and abyssal sediment transport is supported by field evidence. Gardner et al. (2018) found that high surface eddy kinetic energy, mean near-bottom kinetic energy, and benthic energy dissipation all overlap with areas containing dense nepheloid layers, many of which were mapped at depths greater than 4000 m. This, in addition to other field studies linking surface current meanders to deep ocean eddies (Andres et al., 2016; Watts et al., 2001), suggests that deep and bottom water masses may be coupled with the activity of overlying surface currents. We hypothesize that some deep contourites will a preserve a signature of upper ocean dynamics in addition to the signature of deep and bottom water masses. The role of energetic surface currents in affecting contourite deposition should be considered along with the configuration of the deep and bottom water masses.

4.4. Discrepancies between numerical simulations and observed features

Regional-scale plots demonstrate that the link between modern contourite occurrence and variable bottom current speeds remains

Please cite this article in press as: Thran, A.C., et al. Controls on the global distribution of contourite drifts: Insights from an eddy-resolving ocean model. Earth Planet. Sci. Lett. (2018), https://doi.org/10.1016/j.epsl.2018.02.044

robust at smaller scales (Fig. 5), where drifts frequently appear beneath shallow currents (e.g., the Florida Current, Fig. 5B), wind-driven currents (e.g., the ACC, Fig. 6C) and density-driven deep western boundary currents (e.g., the Atlantic and Pacific DWBCs, Fig. 5A, Fig. 7A). Additionally, drifts are present in areas known to experience dense-shelf cascading of newly-formed deep water masses (e.g., the NAdDW in the Adriatic Sea, Fig. 5C). We reiterate the importance of local topography in the redirection and modification of current intensities in all regions, where smaller-scale features can be present. However, our numerical simulations are inconsistent with a small number of contourite occurrences.

The widely-known Gloria Drift in the Northern North Atlantic experiences markedly low simulated current activity (#31 – Fig. 5A). Current meter measurements in the area confirm this relatively quiescent setting (Egloff and Johnson, 1975). While very little is known regarding the drift's recent (<1 Ma) depositional history, Egloff and Johnson (1975) suggest that the Gloria Drift may be a surficial but relict feature of paleocirculation pathways in the North Atlantic, and is no longer undergoing deposition. Therefore, there are drifts within our compilation that could still manifest surficially with minor on-going accumulation (i.e., in a more mature "drift maintenance" stage), with their main drift-building stage reflecting an extinct configuration of paleocurrent routes. This also appears to be the case for a cluster of drifts located east of New Zealand (Fig. 7A), some of which are thought to have been more active during glacial periods (McCave and Carter, 1997).

In addition, our model produces lower than expected current activity over a cluster of small drifts on the northern slope of the South China Sea (Fig. 7B). Other regional numerical models indicate that while lateral unidirectional currents may be less energetic, tidal flows may produce bottom current speeds that surpass the necessary threshold for re-mobilising sediment in this area (i.e., 15 cm/s; Chen et al., 2016). Tidal flows are not explicitly resolved in the MOM01 ocean model, with tidal mixing effects parameterized.

4.5. Notable regions for future investigation

Given the paleoceanographic and paleoclimatic significance of contourite drifts (Rebesco et al., 2014), this work presents a new opportunity to identify new drilling targets for as-of-yet undiscovered modern drifts. There are numerous areas globally where vigorous bottom current activity is simulated and contourites have not been documented. We briefly highlight a few main regions.

A standout region is the Kerguelen Plateau, a Large Igneous Province that obstructs and redirects bottom water flow (Fig. 4A; Fukamachi et al., 2010). Sparse ocean drilling data at this location suggest the presence of drifts on the eastern side of the plateau (Joseph et al., 2002) and on the Southeast Indian Ridge (Dezileau et al., 2000), though this requires confirmation from sub-bottom profiling. Contourites in this region could provide high-resolution records that contain new insights into the paleoceanographic history of the ACC and AABW, as the majority of knowledge of these water masses stems from surveys in the South Atlantic.

Another area which could host modern sediment drifts is the Indonesian Archipelago (Fig. 4A), a region of profound oceanographic and climatic significance as the principle site for Indonesian Throughflow. Neogene tectonic and paleobathymetric reconstructions suggest that this region operated as an important ocean gateway that allowed deep water exchange between the western Pacific and eastern Indian oceans (Gaina and Müller, 2007). Potential contourite drifts in this area would similarly help inform and refine the history of paleo-throughflow.

Other areas of note which show high eddy kinetic energy and lie within relatively close proximity to terrestrial or volcanic sediment sources include the Bering Sea, Southwest Greenland, the southern Caribbean Sea, the Barents Sea, the East African continental margin, Cooperation Sea, the Shatsky Rise, and the Torres Strait in northern Australia (Fig. 4A). Some of the areas exhibiting vigorous bottom current activity in the Southern Ocean have been attributed to present-day unconformity fields (Dutkiewicz et al., 2016), though these regions could potentially be interspersed with areas of modern deposition of pelagic sediment.

4.6. Recommendations for areas of future work on contourite drifts

Future work would greatly benefit from the implementation of partial or fully-coupled sediment-transport models, which would help to more firmly establish robust causal mechanisms. Regional drift-modelling studies that incorporate sediment transport dynamics reveal model sensitivities to supply factors such as downslope transport of shelf-derived material and particle parameters such as density and grain size, which affect suspended load flux (Haupt et al., 1994; Salles et al., 2010). Additional fieldwork highlights the importance of "sediment-laden" water in the construction and maintenance of sediment drifts (Hollister and McCave, 1984; Hunter et al., 2007). Our preliminary results are promising, as they demonstrate a clear, directly proportional relationship between current intensity and principle grain sizes of the drifts (Fig. 3). However, such relationships between critical bed shear, suspended load transport, and selective deposition may not be as clear-cut as previously thought and might require site-specific calibration (McCave et al., 2017). This will be particularly important in understanding the delicate balance between constructive and deleterious impacts on the deep-sea sedimentological record (Dutkiewicz et al., 2016). Future work would require a more thorough examination of sediment properties and at feature-specific scales, along with a more rigorous quantification of sediment sources and sinks in areas with known contouritic deposition.

Additionally, our results help to illustrate the importance of eddies in instigating vigorous bottom activity. However, regional violin plots suggest that they might not be as important for some areas (e.g. the Eastern North Atlantic) as they are for others (e.g. the Western South Atlantic; Fig. 4B). This may be due to a bias of model resolution. Contourites in areas of low simulated eddy kinetic energy, such as the Northwest Pacific (i.e., the South China Sea) and the Eastern North Atlantic (i.e., the Iberian Peninsula) tend to be comparatively small (see Supplementary Table S1 for computed areas), and the model might not permit eddies to be captured at those scales. Nevertheless, it is also possible that other mechanisms are simply more influential in these areas, and future work should continue to investigate and numerically capture the myriad of oceanographic processes that are believed to trigger high-intensity fluctuations in current flow. Of the lesser-known phenomena, internal waves and "pulse-like" ocean density fronts, arise from instabilities at the interface between highly stratified layers and are hypothesized to play a role in localised drift sedimentation (Droghei et al., 2016; Hanebuth et al., 2015). On a larger scale, identifying factors that drive long-term alterations to the intensity and configuration of global MOC, which provides a necessary backdrop for fluctuations in mean flow, will be equally important. Finally, there is enormous potential for the implementation of paleo-ocean circulation models in identifying relict/buried features that could provide invaluable insight into past paleoceanographic and paleoclimatic changes. Such challenges can only be achieved via an interdisciplinary approach to reconstructing contourite depositional histories and disentangling the various processes that control their formation (Rebesco et al., 2014).

Please cite this article in press as: Thran, A.C., et al. Controls on the global distribution of contourite drifts: Insights from an eddy-resolving ocean model. Earth Planet. Sci. Lett. (2018), https://doi.org/10.1016/j.epsl.2018.02.044

5. Conclusions

This study demonstrates a robust link between contourite occurrence and vigorous bottom current activity through the use of newly-updated contourite coverage and high-performance numerical ocean modelling. We show that global MOC exerts first-order control on the global distribution of drifts. Bathymetry additionally regulates and modifies flow, resulting in contourite deposition on a wide range of spatial scales. On average, areas with contourite coverage do not achieve speeds that are capable of continuously re-entraining sediment throughout the year (2.2 cm/s). However, contourite-covered areas experience much higher maximum speeds and degrees of fluctuation than the rest of the ocean. This suggests that high-energy, intermittent events interspersed with low ambient flow are responsible for building drifts, where such bursts in speed in the present model are principally caused by the transient flow of eddies. Care must be taken when interpreting the deep-sea sedimentological record, as contourite drift development might not reflect an overall increase in background current flow, but rather an overall increase in susceptibility to repeated, exceptional events. We also note the potential influence of surface currents in mediating abyssal sediment transport processes through the action of deep eddy circulation. Future work should quantitatively explore the associated sediment transport dynamics that may influence drift sedimentation, and should continue to investigate the role of eddies and other mechanisms in triggering high-speed current events.

Author Contributions A.D. conceived the study and designed it with A.T., who collated the database. P.S. produced the model results. A.T. and P.S. conducted the analysis. A.T. wrote the initial manuscript with further development and input from A.D., R.D.M., and P.S.

Acknowledgements

We thank the Flanders Marine Institute, Michele Rebesco, and Francisco Hernández-Molina for graciously permitting us to utilize and reproduce portions of their databases for this work. We are grateful to Lyndon Hall, who provided technical assistance in fine-tuning contourite coverage, and Kial Stewart, who computed the eddy kinetic energies used in our analysis. We also thank Simon Williams for technical assistance and fruitful discussions. This project was supported by the DBH Scholarship (Thran), the University of Sydney Faculty of Science Seed Grant (Dutkiewicz), and the Australian Research Council (ARC) ITRP grant IH130200012 (Müller). P. Spence was supported by an ARC DECRA Fellowship DE150100223. Computing services were provided by the National Computational Infrastructure (NCI) in Canberra, Australia, which is supported by the Australian Commonwealth Government. We are grateful to Lara Pérez and Wilford Gardner for their careful reviews of our manuscript and their constructive comments. We also thank the editor, Martin Frank.

Appendix A. Supplementary material

Supplementary material related to this article can be found online at https://doi.org/10.1016/j.epsl.2018.02.044.

References

Andres, M., Toole, J.M., Torres, D.J., Smethie, W.M., Joyce, T.M., Curry, R.G., 2016. Stirring by deep cyclones and the evolution of Denmark strait overflow water observed at line W. Deep-Sea Res., Part 1, Oceanogr. Res. Pap. 109, 10–26. https://doi.org/10.1016/j.dsr.2015.12.011.

Bonaldo, D., Benetazzo, A., Bergamasco, A., Campiani, E., Foglini, F., Sclavo, M., Trincardi, F., Carniel, S., 2016. Interactions among Adriatic continental margin morphology, deep circulation and bedform patterns. Mar. Geol. 375, 82–98. https://doi.org/10.1016/j.margeo.2015.09.012.

Bower, A.S., Hunt, H.D., 2000. Lagrangian observations of the deep western boundary current in the North Atlantic Ocean. Part I: large-scale pathways and spreading rates. J. Phys. Oceanogr. 30, 764–783. https://doi.org/10.1175/1520-0485(2000)030<0764:LOOTDW>2.0.CO;2.

Breitzke, M., Wiles, E., Krocker, R., Watkeys, M.K., Jokat, W., 2017. Seafloor morphology in the Mozambique channel: evidence for long-term persistent bottom-current flow and deep-reaching eddy activity. Mar. Geophys. Res. 38, 241–269. https://doi.org/10.1007/s11001-017-9322-7.

Carter, L., Carter, R.M., McCave, I.N., 2004. Evolution of the sedimentary system beneath the deep Pacific inflow off eastern New Zealand. Mar. Geol. 205, 9–27. https://doi.org/10.1016/S0025-3227(04)00016-7.

Chen, H., Xie, X., Zhang, W., Shu, Y., Wang, D., Vandorpe, T., Van Rooij, D., 2016. Deep-water sedimentary systems and their relationship with bottom currents at the intersection of Xisha Trough and Northwest Sub-Basin, South China Sea. Mar. Geol. 378, 101–113. https://doi.org/10.1016/j.margeo.2015.11.002.

Claus, S., De Hauwere, N., Vanhoorne, B., Hernandez, F., Mees, J., 2017. MarineRegions.org [WWW Document]. URL MarineRegions.org (accessed 9.15.17).

Dezileau, L., Bareille, G., Reyss, J.L., Lemoine, F., 2000. Evidence for strong sediment redistribution by bottom currents along the southeast Indian ridge. Deep-Sea Res., Part 1, Oceanogr. Res. Pap. 47, 1899–1936. https://doi.org/10.1016/S0967-0637(00)00008-X.

Droghei, R., Falcini, F., Casalbore, D., Martorelli, E., Mosetti, R., Sannino, G., Santoleri, R., Chiocci, F.L., 2016. The role of internal solitary waves on deep-water sedimentary processes: the case of up-slope migrating sediment waves off the Messina Strait. Sci. Rep. 6, 36376. https://doi.org/10.1038/srep36376.

Dutkiewicz, A., Müller, R.D., Hogg, A.M., Spence, P., 2016. Vigorous deep-sea currents cause global anomaly in sediment accumulation in the Southern Ocean. Geology 44, G38143.1. https://doi.org/10.1130/G38143.1.

Egloff, J., Johnson, G.L., 1975. Morphology and structure of the southern Labrador Sea. Can. J. Earth Sci. 12, 2111–2133. https://doi.org/10.1139/e75-186.

Faugères, J.-C., Lima, A.F., Massé, L., Zaragosi, S., 2002. The Columbia channel-levee system: a fan drift in the southern Brazil Basin. Mem. Geol. Soc. Lond. 22, 223–238. https://doi.org/10.1144/GSL.MEM.2002.022.01.16.

Flood, R.D., Shor, A.N., 1988. Mud waves in the Argentine Basin and their relationship to regional bottom circulation patterns. Deep-Sea Res., Part 1, Oceanogr. Res. Pap. 35, 943–971. https://doi.org/10.1016/0198-0149(88)90070-2.

Fukamachi, Y., Rintoul, S.R., Church, J.A., Aoki, S., Sokolov, S., Rosenberg, M.A., Wakatsuchi, M., 2010. Strong export of Antarctic Bottom Water east of the Kerguelen plateau. Nat. Geosci. 3, 327. https://doi.org/10.1038/ngeo842.

Gaina, C., Müller, D., 2007. Cenozoic tectonic and depth/age evolution of the Indonesian gateway and associated back-arc basins. Earth-Sci. Rev. 83, 177–203. https://doi.org/10.1016/j.earscirev.2007.04.004.

Gardner, W.D., Richardson, M.J., Mishonov, A.V., 2018. Global assessment of benthic nepheloid layers and linkage with upper ocean dynamics. Earth Planet. Sci. Lett. 482, 126–134.

Gardner, W.D., Tucholke, B.E., Richardson, M.J., Biscaye, P.E., 2017. Benthic storms, nepheloid layers, and linkage with upper ocean dynamics in the western North Atlantic. Mar. Geol. 385, 304–327. https://doi.org/10.1016/j.margeo.2016.12.012.

Gorski, K.M., Hivon, E., Banday, A.J., Wandelt, B.D., Hansen, F.K., Reinecke, M., Bartelmann, M., 2005. HEALPix: a framework for high-resolution discretization and fast analysis of data distributed on the sphere. Astrophys. J. 622, 759–771. https://doi.org/10.1086/427976.

Griffies, S.M., Biastoch, A., Böning, C., Bryan, F., Danabasoglu, G., Chassignet, E.P., England, M.H., Gerdes, R., Haak, H., Hallberg, R.W., Hazeleger, W., Jungclaus, J., Large, W.G., Madec, G., Pirani, A., Samuels, B.L., Scheinert, M., Gupta, Sen, A., Severijns, C.A., Simmons, H.L., Treguier, A.M., Winton, M., Yeager, S., Yin, J., 2009. Coordinated Ocean-ice Reference Experiments (COREs). Ocean Model. 26, 1–46. https://doi.org/10.1016/j.ocemod.2008.08.007.

Griffies, S.M., Winton, M., Anderson, W.G., Benson, R., Delworth, T.L., Dufour, C.O., Dunne, J.P., Goddard, P., Morrison, A.K., Rosati, A., Wittenberg, A.T., Yin, J., Zhang, R., 2015. Impacts on ocean heat from transient mesoscale eddies in a hierarchy of climate models. J. Climate 28, 952–977. https://doi.org/10.1175/JCLI-D-14-00353.1.

Gross, T.F., Williams, A.J., 1991. Characterization of deep-sea storms. Mar. Geol. 99, 281–301. https://doi.org/10.1016/0025-3227(91)90045-6.

Hanebuth, T.J.J., Zhang, W., Hofmann, A.L., Löwemark, L.A., Schwenk, T., 2015. Oceanic density fronts steering bottom-current induced sedimentation deduced from a 50 ka contourite-drift record and numerical modeling (off NW Spain). Quat. Sci. Rev. 112, 207–225. https://doi.org/10.1016/j.quascirev.2015.01.027.

Haupt, B.J., Schäfer-Neth, C., Stattegger, K., 1994. Modeling sediment drifts: a coupled oceanic circulation-sedimentation model of the northern North Atlantic. Paleoceanography 9, 897–916. https://doi.org/10.1029/94PA01437.

Heezen, B.C., Hollister, C.D., Ruddiman, W.F., 1966. Shaping of the continental rise by deep geostrophic contour currents. Science. https://doi.org/10.1126/science.152.3721.502.

Hernández-Molina, F.J., Paterlini, M., Violante, R., Marshall, P., de Isasi, M., Somoza, L., Rebesco, M., 2009. Contourite depositional system on the Argentine Slope:

Please cite this article in press as: Thran, A.C., et al. Controls on the global distribution of contourite drifts: Insights from an eddy-resolving ocean model. Earth Planet. Sci. Lett. (2018), https://doi.org/10.1016/j.epsl.2018.02.044

an exceptional record of the influence of Antarctic water masses. Geology 37, 507–510. https://doi.org/10.1130/G25578A.1.

Hernández-Molina, F.J., Serra, N., Stow, D.A.V., Llave, E., Ercilla, G., Van Rooij, D., 2011. Along-slope oceanographic processes and sedimentary products around the Iberian margin. Geo Mar. Lett. 31, 315–341. https://doi.org/10.1007/s00367-011-0242-2.

Hillenbrand, C.-D., Camerlenghi, A., Cowan, E.A., Hernández-Molina, F.J., Lucchi, R.G., Rebesco, M., Uenzelmann-Neben, G., 2008. The present and past bottom-current flow regime around the sediment drifts on the continental rise West of the Antarctic Peninsula. Mar. Geol. 255, 55–63. https://doi.org/10.1016/j.margeo.2008.07.004.

Hollister, C.D., Heezen, B.C., 1972. Geologic effects of ocean bottom currents: western North Atlantic. In: Gordon, A.L. (Ed.), Studies in Physical Oceanography. Gordon and Breach, New York, pp. 37–66.

Hollister, C.D., McCave, I.N., 1984. Sedimentation under deep-sea storms. Nature 309, 220–225. https://doi.org/10.1038/309220a0.

Hunter, S., Wilkinson, D., Louarn, E., McCave, I.N., Rohling, E., Stow, D.A.V., Bacon, S., 2007. Deep western boundary current dynamics and associated sedimentation on the Eirik Drift, Southern Greenland Margin. Deep-Sea Res., Part 1, Oceanogr. Res. Pap. 54, 2036–2066. https://doi.org/10.1016/j.dsr.2007.09.007.

Joseph, L.H., Rea, D.K., van der Pluijm, B.A., Gleason, J.D., 2002. Antarctic environmental variability since the late Miocene: ODP Site 745, the East Kerguelen sediment drift. Earth Planet. Sci. Lett. 201, 127–142. https://doi.org/10.1016/S0012-821X(02)00661-1.

Laberg, J.S., Dahlgren, T., Vorren, T.O., Haflidason, H., Bryn, P., 2001. Seismic analyses of Cenozoic contourite drift development in the Northern Norwegian Sea. Mar. Geophys. Res. 22, 401–416. https://doi.org/10.1023/A:1016347632294.

Li, H., Wang, Y., Zhu, W., Xu, Q., He, Y., Tang, W., Zhuo, H., Wang, D., Wu, J., Li, D., 2013. Seismic characteristics and processes of the Plio-Quaternary unidirectionally migrating channels and contourites in the northern slope of the South China Sea. Mar. Pet. Geol. 43, 370–380. https://doi.org/10.1016/j.marpetgeo.2012.12.010.

Martorelli, E., Falcini, F., Salusti, E., Chiocci, F.L., 2010. Analysis and modeling of contourite drifts and contour currents off promontories in the Italian Seas (Mediterranean Sea). Mar. Geol. 278, 19–30. https://doi.org/10.1016/j.margeo.2010.08.007.

Mauritzen, C., Polzin, K.L., McCartney, M.S., Millard, R.C., West-Mack, D.E., 2002. Evidence in hydrography and density fine structure for enhanced vertical mixing over the Mid-Atlantic Ridge in the western Atlantic. J. Geophys. Res., Oceans 107, 11–19. https://doi.org/10.1029/2001JC001114.

McCave, I.N., Carter, L., 1997. Recent sedimentation beneath the deep Western Boundary Current off northern New Zealand. Deep-Sea Res., Part 1, Oceanogr. Res. Pap. 44, 1203–1237. https://doi.org/10.1016/S0967-0637(97)00011-3.

McCave, I.N., Hall, I.R., 2006. Size sorting in marine muds: processes, pitfalls, and prospects for paleoflow-speed proxies. Geochem. Geophys. Geosyst. 7. https://doi.org/10.1029/2006GC001284.

McCave, I.N., Thornalley, D.J.R., Hall, I.R., 2017. Relation of sortable silt grain-size to deep-sea current speeds: Calibration of the "Mud Current Meter.". Deep-Sea Res., Part 1, Oceanogr. Res. Pap. 127, 1–12. https://doi.org/10.1016/j.dsr.2017.07.003.

McCave, I.N., Tucholke, B.E., 1986. Deep current-controlled sedimentation in the western North Atlantic. In: Vogt, P.R., Tucholke, B.E. (Eds.), The Geology of North America, Volume M: the Western North Atlantic Region. The Geological Society of America, Boulder, Colorado, pp. 451–468.

Millot, C., 1999. Circulation in the western Mediterranean Sea. J. Mar. Syst. 20, 423–442. https://doi.org/10.1016/S0924-7963(98)00078-5.

Orsi, A.H., Whitworth, T., Nowlin, W.D., 1995. On the meridional extent and fronts of the Antarctic Circumpolar Current. Deep-Sea Res., Part 1, Oceanogr. Res. Pap. 42, 641–673. https://doi.org/10.1016/0967-0637(95)00021-W.

Pérez, L.F., Hernández-Molina, F.J., Esteban, F.D., Tassone, A., Piola, A.R., Maldonado, A., Preu, B., Violante, R.A., Lodolo, E., 2015. Erosional and depositional contourite features at the transition between the western Scotia Sea and southern South Atlantic Ocean: links with regional water-mass circulation since the Middle Miocene. Geo Mar. Lett. 35, 271–288. https://doi.org/10.1007/s00367-015-0406-6.

Rebesco, M., Hernández-Molina, F.J., van Rooij, D., Wahlin, A., 2014. Contourites and associated sediments controlled by deep-water circulation processes: state-of-the-art and future considerations. Mar. Geol. 352, 111–154. https://doi.org/10.1016/j.margeo.2014.03.011.

Rebesco, M., Wåhlin, A., Laberg, J.S., Schauer, U., Beszczynska-Möller, A., Lucchi, R.G., Noormets, R., Accettella, D., Zarayskaya, Y., Diviacco, P., 2013. Quaternary contourite drifts of the Western Spitsbergen margin. Deep-Sea Res., Part 1, Oceanogr. Res. Pap. 79, 156–168. https://doi.org/10.1016/j.dsr.2013.05.013.

Salles, T., Marchès, E., Dyt, C., Griffiths, C., Hanquiez, V., Mulder, T., 2010. Simulation of the interactions between gravity processes and contour currents on the Algarve Margin (South Portugal) using the stratigraphic forward model Sedsim. Sediment. Geol. 229, 95–109. https://doi.org/10.1016/j.sedgeo.2009.05.007.

Schattner, U., Gurevich, M., Kanari, M., Lazar, M., 2015. Levant jet system—effect of post LGM seafloor currents on Nile sediment transport in the eastern Mediterranean. Sediment. Geol. 329, 28–39. https://doi.org/10.1016/j.sedgeo.2015.09.007.

Spence, P., Saenko, O.A., Sijp, W., England, M., 2012. The role of bottom pressure torques on the interior pathways of North Atlantic Deep Water. J. Phys. Oceanogr. 42, 110–125. https://doi.org/10.1175/2011JPO4584.1.

Stewart, K.D., Hogg, A.M., Griffies, S.M., Heerdegen, A.P., Ward, M.L., Spence, P., England, M.H., 2017. Vertical resolution of baroclinic modes in global ocean models. Ocean Model. 113, 50–65. https://doi.org/10.1016/j.ocemod.2017.03.012.

Stow, D.A.V., Faugères, J.-C., Howe, J.A., Pudsey, C.J., Viana, A.R., 2002. Bottom currents, contourites and deep-sea sediment drifts: current state-of-the-art. Mem. Geol. Soc. Lond. 22, 7–20.

Stow, D.A.V., Hernández-Molina, F.J., Llave, E., Sayago-Gil, M., Díaz, V., Branson, A., 2009. Bedform-velocity matrix: the estimation of bottom current velocity from bedform observations. Geology 37, 327–330. https://doi.org/10.1130/G25259A.1.

Uenzelmann-Neben, G., Weber, T., Grützner, J., Thomas, M., 2016. Transition from the Cretaceous ocean to Cenozoic circulation in the western South Atlantic—a twofold reconstruction. Tectonophysics 716, 225–240. https://doi.org/10.1016/j.tecto.2016.05.036.

Watts, D.R., Qian, X., Tracey, K.L., 2001. Mapping abyssal current and pressure fields under the meandering Gulf Stream. J. Atmos. Ocean. Technol. 18, 1052–1067.

Wold, C.N., 1994. Cenozoic sediment accumulation on drifts in the northern North Atlantic. Paleoceanography 9, 917–941. https://doi.org/10.1029/94PA01438.

Wong, H.K., Lüdmann, T., Baranov, B.V., Karp, B.Y., Konerding, P., Ion, G., 2003. Bottom current-controlled sedimentation and mass wasting in the northwestern Sea of Okhotsk. Mar. Geol. 201, 287–305. https://doi.org/10.1016/S0025-3227(03)00221-4.

Zhang, W., Hanebuth, T.J.J., Stöber, U., 2016. Short-term sediment dynamics on a meso-scale contourite drift (off NW Iberia): impacts of multi-scale oceanographic processes deduced from the analysis of mooring data and numerical modelling. Mar. Geol. 378, 81–100. https://doi.org/10.1016/j.margeo.2015.12.006.

Please cite this article in press as: Thran, A.C., et al. Controls on the global distribution of contourite drifts: Insights from an eddy-resolving ocean model. Earth Planet. Sci. Lett. (2018), https://doi.org/10.1016/j.epsl.2018.02.044

XMLVIEW: extended

Appendix A. Supplementary material

The following is the Supplementary material related to this article.

begin ecomponent begin ecomponent begin ecomponent begin ecomponent begin ecomponent begin ecomponent begin ecomponent begin ecomponent begin ecomponent begin ecomponent begin ecomponent begin ecomponent begin ecomponent begin ecomponent begin ecomponent begin ecomponent begin ecomponent begin ecomponent

Label: MMC 1
caption: Contourite attributes.
link: **APPLICATION : mmc1**

end ecomponent end ecomponent end ecomponent end ecomponent end ecomponent end ecomponent end ecomponent end ecomponent end ecomponent end ecomponent end ecomponent end ecomponent end ecomponent end ecomponent end ecomponent end ecomponent end ecomponent end ecomponent end ecomponent
begin ecomponent begin ecomponent begin ecomponent begin ecomponent begin ecomponent begin ecomponent begin ecomponent begin ecomponent begin ecomponent begin ecomponent begin ecomponent begin ecomponent begin ecomponent begin ecomponent begin ecomponent begin ecomponent begin ecomponent begin ecomponent

Label: MMC 2
caption: Supplementary References for Table S1.
link: **APPLICATION : mmc2**

end ecomponent end ecomponent end ecomponent end ecomponent end ecomponent end ecomponent end ecomponent end ecomponent end ecomponent end ecomponent end ecomponent end ecomponent end ecomponent end ecomponent end ecomponent end ecomponent end ecomponent end ecomponent end ecomponent

Google maps

The following KML file contains the Google map of the most important areas described in this article.

begin ecomponent begin ecomponent begin ecomponent begin ecomponent begin ecomponent begin ecomponent begin ecomponent begin ecomponent begin ecomponent begin ecomponent begin ecomponent begin ecomponent begin ecomponent begin ecomponent begin ecomponent begin ecomponent begin ecomponent begin ecomponent

Label: Map
caption: Contourite polygons used to extract various modelled bottom current metrics. Features were compiled from an online database curated by the Flanders Marine Institute (Claus et al., 2017; marine regions.org), a recent review of contourites (Rebesco et al., 2014), and an additional review of the literature. Coverage of each feature was delineated and/or verified using georeferenced figures from their relevant publications. More attributes for each feature (e.g., maximum age, morphological characteristics, principle grain size, area, and computed bottom current metrics), along with their key references, may be found in Supplementary Table S1. Features were omitted if they were identified solely on the basis of sediment cores or if they are presently buried.
link: **APPLICATION : mmc3**

end ecomponent end ecomponent end ecomponent end ecomponent end ecomponent end ecomponent end ecomponent end ecomponent end ecomponent end ecomponent end ecomponent end ecomponent end ecomponent end ecomponent end ecomponent end ecomponent end ecomponent end ecomponent end ecomponent

---

Please cite this article in press as: Thran, A.C., et al. Controls on the global distribution of contourite drifts: Insights from an eddy-resolving ocean model. Earth Planet. Sci. Lett. (2018), https://doi.org/10.1016/j.epsl.2018.02.044

Sponsor names

Do not correct this page. Please mark corrections to sponsor names and grant numbers in the main text.

Q7 **Australian Research Council**, *country*=Australia, *grants*=IH130200012

Please cite this article in press as: Thran, A.C., et al. Controls on the global distribution of contourite drifts: Insights from an eddy-resolving ocean model. Earth Planet. Sci. Lett. (2018), https://doi.org/10.1016/j.epsl.2018.02.044

Highlights

- Western boundary currents and MOC dictate global contourite distribution.
- Mean bottom current speeds fall below proposed thresholds for entraining sediment.
- Bottom currents reach higher maximum speeds and fluctuate more over contourites.
- Fluctuations in bottom current speeds are principally caused by eddies.
- Contourites may preserve a signature of upper ocean dynamics.

Please cite this article in press as: Thran, A.C., et al. Controls on the global distribution of contourite drifts: Insights from an eddy-resolving ocean model. Earth Planet. Sci. Lett. (2018), https://doi.org/10.1016/j.epsl.2018.02.044